Assessing hybrid supercapacitor-battery energy storage for active power management in a wind-diesel system

Assessing Hybrid Supercapacitor-Battery Energy Storage for Active Power Management in a Wind-Diesel System

H. Shayeghi [1,*], F. Monfaredi [1], A. Dejamkhooy [1], M. Shafie-khah [2], J.P.S. Catalão [3,*]

[1] *Department of Technical Engineering, University of Mohaghegh Ardabili, Ardabil, Iran*

[2] *School of Technology and Innovations, University of Vaasa, Vaasa, Finland*

[3] *Faculty of Engineering of University of Porto and INESC TEC, Porto, Portugal*

Abstract-This paper presents an effective hybrid supercapacitor-battery energy storage system (SC-BESS) for the active power management in a wind-diesel system using a fuzzy type distributed control system (DCS) to optimally regulate the system transient. It addresses a new online intelligent approach by using a combination of the fuzzy logic and DCS based on the particle swarm optimization techniques for optimal tuning and reduce the design effort of the control system. This mechanism combines the features of online fuzzy theory and distributed control system (DOFCS), which has a flexible structure. The proposed energy management algorithm for the hybrid SC-BESS is well able to repel the peak-impact of the battery storage system during the wind speed and load changes. The high performance of the suggested methodology is represented on a typical wind-diesel test system.

Keywords-Hybrid energy storage; Power management; Distributed control system; Battery energy storage; Wind diesel system.

*Corresponding authors: hshayeghi@gmail.com (H. Shayeghi) and catalao@fe.up.pt (J.P.S. Catalão)

Nomenclature

WTG	Wind turbine generator	ESS	Energy storage system
DOFCS	Distributed online fuzzy control system	DG	Diesel generator
SC	Supercapacitor	PSO	Particle swarm optimization
BESS	Battery energy storage system	DCS	Distributed control system
SOC	State of charge	SOC_0	Initial SOC value of battery
IG	Induction generator	DE	Diesel engine
SG	Synchronous generator	CCI	Current controlled inverter
APR	Active power regulator	PV	Photovoltaic
P_L	Load consumed active power	P_T	WTG generated active power
Q_L	Load consumed reactive power	Q_T	The WTG generated reactive power
P_S	The BESS consumed/supplied active power	Q_S	The BESS consumed/supplied reactive power
P_{SG}	The SG generated active power	Q_{SG}	The SG generated reactive power
I_{SG}	SG current	V_{SG}	SG voltage
P_{REF}	Reference power for balancing the active power	f_{NOM}	Rated frequency of the system
f	Actual frequency	e_f	Frequency error
P_{INV}	The BESS consumed power	E_0	Constant voltage
K	Polarization constant (Ah^{-1})	i^*	Current dynamics in Low frequency (A)
i_b	Battery current (A)	t	Time (s)
Q	Maximum battery capacity (Ah)	Q_n	Battery rated capacity
A	Exponential voltage (V)	B	Exponential zone time constant, (Ah^{-1})
R	Internal resistance (Ω)	η	Coulomb efficiency
V_{SC}	Output voltage of SC (V)	i_{SC}	Output current of SC (A)
α_i	SC voltage rates of change	A_i	Electrodes and electrolyte between interfacial area
it	Actual battery charge (Ah)		(m^2)
C_m	Molar concentration (mol/m^3)	R_d	Molecular radius (m)
F	Faraday constant	C_T	Total capacitance (F)
R_{SC}	Total resistance (ohms)	N_e	Number of layers of electrodes
N_A	Avogadro constant	N_{pc}	Number of parallel SCs
N_{sc}	Number of series SCs	Q_{ec}	Electric charge (C)
pu	Per unit	D	Molecular radius
T	Operating temperature (K)	ε	Permittivity of material
ε_0	Permittivity of free space	Ki	Integral gain
K_P	Proportional gain	K_D	Derivative gain

P_{DE}	Mechanical power supplied by the DE	J	DG inertia
ω	Shaft speed	e_P	Power error SG
V_b	Ideal voltage source	R_b	Internal resistance
C	Single lumped constant capacitance	s	Complex frequency
R_c	C together with an internal lumped resistance	Φ (t)	Unit step function
V_{c0}	Initial voltage of the SC	ζ_c	Current sharing factor of the SC at the peak charging
I_0	Amplitude of the charging/load current		current

1. Introduction

In remote environmental zones, where the main power network grid is not available, a local microgrid is combined with the conventional diesel generator and renewable sources can be recognized [1]. A combination of the wind turbine with diesel generator is usually used to find maximum influence of the discontinuous wind source in the generated total power [2]. The key task of renewable sources is their randomness and changeability nature in the generated power. Regarding these features, the main problem for researchers is power quality keeping and power supply changes minimizing or system frequency regulation in the microgrid.

Different solutions to deal with the frequency oscillation problem are investigated in the microgrid [3]. To control the system frequency in the desired level, extra rotating masses are added in this solution for increasing inertia of the microgrid. For control of the microgrid frequency a dynamic strategy was used in the French island of Guadeloupe to enlarge penetration of the clean power [4]. In [5], using the PSO technique a multi part fuzzy controller was presented for frequency control. Shayeghi and Younesi [6] suggested an adaptive two-stage controller for an isolated microgrid using the reinforcement learning method. The first stage has a PID controller and the second stage has a reinforcement learning type controller that its performance was continuously updated due to the transient variations in the microgrid.

In [7] a complex FuzzyP+FuzzyI+FuzzyD controller was designed for simultaneous control of the voltage/frequency in a microgrid. The authors attempted to determine the optimal control

gains and fuzzy membership functions using an improved Salp swarm algorithm to achieve optimal dynamic response. In [8], metaheuristic optimization algorithm, the Hopfield fuzzy neural network method was applied to regulate frequency deviation. Using the future production densities obtained from a probabilistic wind speed forecast, an operational strategy for the management of a set of batteries connected to a wind-farm was suggested in [9] to stochastic model predictive control of the deviations from the dispatch curve. In [10], a coordinated control strategy for a microgrid with hybrid energy resources and ac/dc loads was reported. A local-level coordinated control strategy of distributed converters was proposed, where a model predictive power and voltage control method was developed for the ac/dc interlinking converter. In [11], a stochastic-heuristic model to minimize the net present cost of stand-alone hybrid PV/wind-diesel with battery storage systems was presented. The stochastic optimization was developed by means of Monte Carlo simulation. The heuristic approach uses genetic algorithms to obtain the optimal system.

One of the important methods for frequency control in the microgrid is proper management of energy storage systems to decrease the peak charge/discharge current of the battery and improved frequency dynamic behaviors.

An ideal ESS should have great power density to track rapid power variations, high energy density to provide independence for the regulation service provider, and lengthier life for maximizing the profit. As a sole ESS is unable to provide these necessities efficiently and economically, thus it is important to combine various ESSs for making a hybrid storage unit. For example, a battery energy storage and a SC can be used to create a hybrid ESS [12, 13].

Some authors presented the wind-diesel hybrid system with an ESS [14, 15]. The role of the BESS in isolated wind-diesel power system was demonstrated in [14] for active power compensation and frequency regulation in wind-battery operation. The motivation for integration of an ESS into a wind energy system is to take into account the total inertia of wind turbine, low

voltage rides through capability, power quality problems, etc. [16]. Furthermore, different kinds of hybrid ESS are introduced in [17-19], where SC and BESS were applied for meeting the large-scale capability requirement and the short term fast-variation power, respectively. The grid-connected hybrid system in [17] was demonstrated a combination of the battery and SC to reduce the voltage and frequency instabilities as a result of variable wind generation. Several vignettes were tested varying the size of the parallel SC bank where the SC handled short variations and the flow battery handled longer variations. Esmaili et. al [18] suggested the low-pass filters to provide a rate-limited demand signal to sensitive power sources with a separate control for regulation the ESS voltage and manage energy usage. A fixed time constant was used in the low-pass filter and so the ESS has the same response for a specific power step across the full load range. However, to improve and ensure the lifespan of both BESS and SC, it is important which both work inside their operating constraints. BESS must work inside its state of charge and current limits and SC inside its voltage and current limits.

Simultaneously, the SC must reply to fast high current signals for BESS lifetime maximizing [20]. In [21], an optimum energy management structure for hybrid SC/battery energy storage was presented. The optimization problem was formulated for minimizing the current fluctuation in the BESS and the energy dissipation observed by SC [21]. In [22], using the fuzzy theory and a low-pass filter a control approach was reported for the hybrid SC/battery energy storage. The BESS peak current demand is minimized using the suggested strategy while the SOC of the SC is considered constant. A complete wind-diesel power system has been studied to illustrate the efficiency of the system and individual modules [23]. Table 1 lists the recent researches on storage power management and the corresponding control methods. However, there is still no study on the application of the disturbed online fuzzy system for hybrid energy storage management to decrease the peak charge/discharge current of the battery and improve frequency transient during changes in load and wind speed.

Table 1. Storage power management and the corresponding control methods

Ref.	Energy source(s)	ESS	Management strategy	Control strategy
[24]	Wind-diesel	Battery	Optimum load	Controllable loads
[25]	Wind-diesel	Battery	Co-ordination strategy	Load side inverter or by diesel generator due to the wind speeds
[23]	Wind-diesel	Battery	Reverse power	Distributed control system
[14]	Wind	Battery/SC	Optimal energy	Filter based controller
[26]	Wind	Battery/SC	Optimal energy	Rule based controller
[27]	PV	Battery/SC	Load predictive energy	Rule based controller
[28]	Wind & PV	Battery/ Hydrogen	Optimal energy	Fuzzy logic controller
[29]	Wind & PV	Battery/ Hydrogen	Optimal energy	Rule based controller
[30]	PV	Battery	Decentralized power	Model predictive control
Proposed study	Wind-diesel	Hybrid SC-Battery	Reverse power	Distributed online fuzzy control system

In this paper, an effective hybrid ESS is proposed for proper management of the reverse power in an islanded wind-diesel system using the distributed online fuzzy control system (DOFCS). This control approach combines the features of fuzzy theory and distributed control to increase filtering effort of load and wind power fluctuations and reduce fuzzy system efforts. On the other hand, optimal tuning of online fuzzy type DCS gains has a key role to realize the robust performance. Consequently, the PSO algorithm is applied for finding a better system control. Finally, an isolated wind-diesel system including consumer load and a hybrid SC-BESS system is modeled and studied. The results depict that the optimized fuzzy type DCS has a good performance. Also, a high percentage of the battery's peak current is reduced in transient situation and the system frequency/voltage is properly regulated from the point of overshoot/undershoot and settling time in comparison with DCS controller.

In summary, the novel contributions of this study are:

- Suggesting an effective distributed online fuzzy control system to enable the suggested hybrid ESS for properly smoothing the load and wind speed variations for the enhancement of the system power quality.
- Using a PSO technique for optimizing the DOFCS controller gains automatically to reduce design effort and cost.
- Significantly reducing battery's peak current in transient situations to maximize the lifespan of the BESS and investigate the active power balancing capability using the proposed management method for energy of the hybrid SC-BESS and control approach.
- Improving the system frequency by methods: a) using the proposed energy management method of the storage section. b) using the proposed microgrid controller. c) combination of the (a) and (b) methods.
- Improving system voltage by using the proposed DOFCS, a good regulation is achieved with significantly reducing overshoot/undershoot than the DCS controller.

The paper is organized as below. Description of the hybrid wind diesel system is given in Sec. 2. The detailed information of battery storage and SC are given in Secs. 3 and 4, respectively. The proposed control is discussed in Sec. 5. The presented energy management mechanism among the battery storage and SC is described in Sec. 6. Section 7 represents the simulation results. Conclusion is given in Sec. 8.

2. The islanded wind/diesel/storage microgrid

A wind/diesel/storage based isolated microgrid is investigated in this paper. Fig. 1 shows the microgrid schematic (see Ref. [23] for more details). The microgrid operation is depended on the quality of power generation and consumption mismatch.

As illustrated in Fig. 1, the prime mover of the synchronous generator (SG) is a diesel engine. The BESS unit composes of a Nickel-Cadmium battery bank, an LC filter, a three-phase current controlled inverter (CCI), and a transformer. The WTG system includes an induction generator that is linked directly to the distribution lines and the wind turbine. In this paper a fixed speed without pitch control for WTG is used as it has robust construction, low cost and simple maintenance and these are important factors in the remote locations of wind diesel system [23]. The consumer load comprises of a 175 kW as the main load and a 125 kW as an extra load.

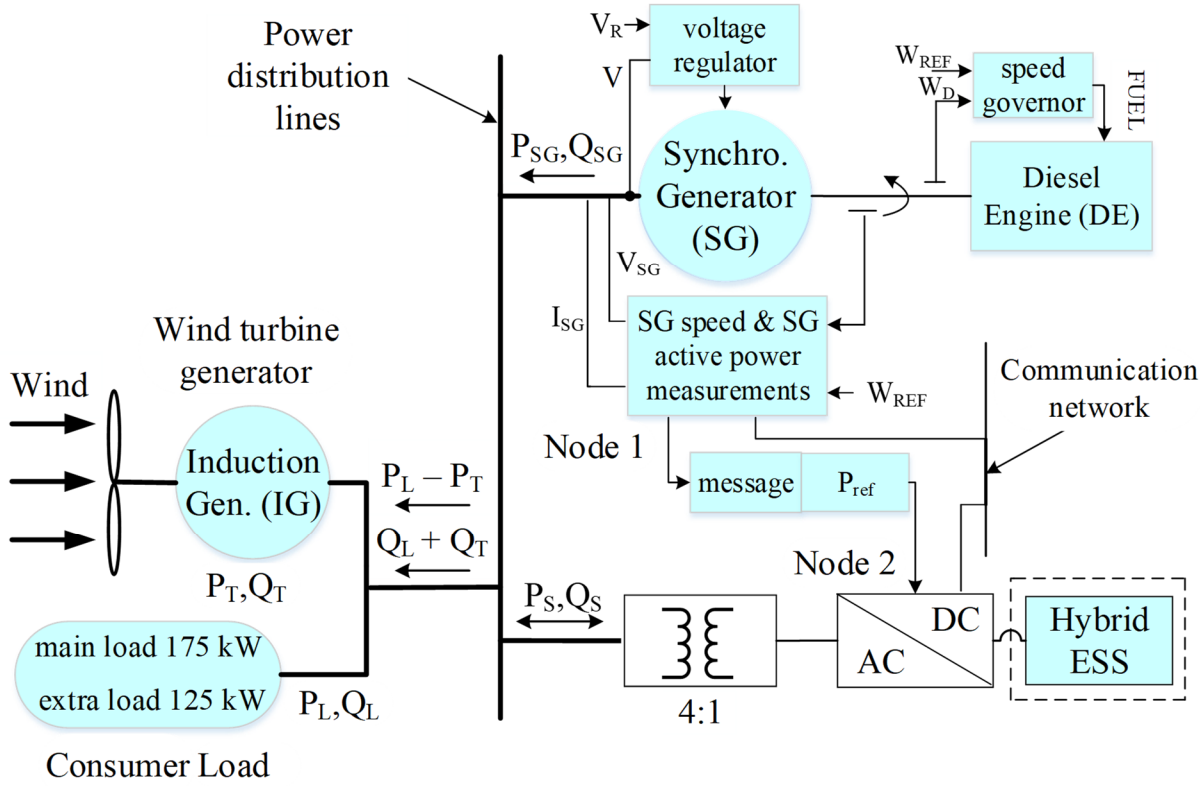

Fig. 1. Overall structure of the studied microgrid.

The active power regulator (APR) (node 1) receives the rotor speed and active power of the SG as inputs. P_{REF} is calculated as:

$$P_{REF} = K_P e_f + K_D \frac{de_f}{dt} + P_{inv} \quad (1)$$

Where, f_{NOM} , f and P_{INV} are the nominal, actual frequency and DE reverse power, respectively and $e_f = f - f_{NOM}$ [23]. The APR controls the system frequency using a discrete PD controller [23].

In Fig. 2, the reverse power protection control is also shown. The dead zone applies an offset to evade extreme action of this control approach. It begins at -6 kW and finishes at 0 kW (2% of $P_{SG\text{-}NOM}$) and $e_P = P_{SG(NOM)} - P_{SG}$. Consequently, once this protection system is actuated the steady state power of DG is retained between 30 to 36 kW. To avoid the reverse power, the wind diesel control system must use the controlled sink/source BESS. If the BESS is added to the power system and being P_S the power consumed/supplied by the BESS (it is considered positive if consumed) then:

$$P_{DE} + P_T - P_L - P_S = J\omega \frac{d\omega}{dt} \quad (2)$$

If we assume that BESS is not in the microgrid ($P_S = 0$), the speed governor (speed regulator and actuator) regulates system frequency by controlling the DE and the diesel speed governor will make the DG run at constant speed ($d\omega/dt = 0$).

The diesel speed governor cannot control P_{DE} if it is out of the range (0, DE rated power) and the 0 lower limit cannot always be satisfied in a wind diesel system. The uncontrolled power generated by the WTG (P_T) can be greater than the consumed power by the load (P_L). As the speed governor cannot order the DE to consume power, it is unable to regulate frequency [23].

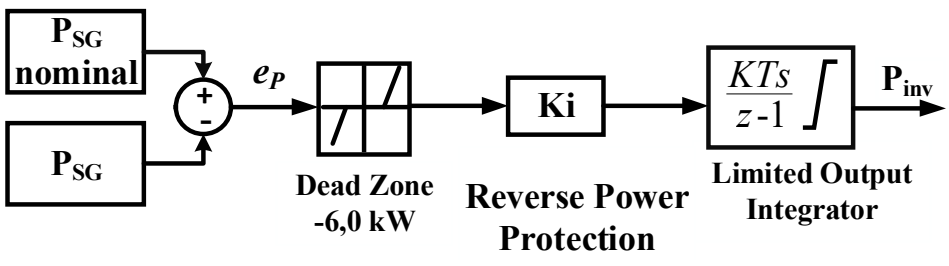

Fig. 2. The protection control scheme for reverse power.

When the produced power of WTG, P_T , is more than load power, P_L, the system active power, P_L - P_T, is negative. Thus, to balance system active power the DG produced power should be negative for regulating the system frequency.

Once the wind speed is high, DG goes to the minimum power production (the min and max DG values are limited) and the BESS begins to charge (production power is more than the consumption power of the microgrid). When the wind speed is low, DG goes to the maximum power production and the BESS begins to discharge. The ESS in Fig. 1 composes of a hybrid SC/battery and DC-DC converter. Fig. 3 shows the structure of the hybrid ESS. ESS and DG performance are dependent on wind power variations. They are compensated for active power shortages.

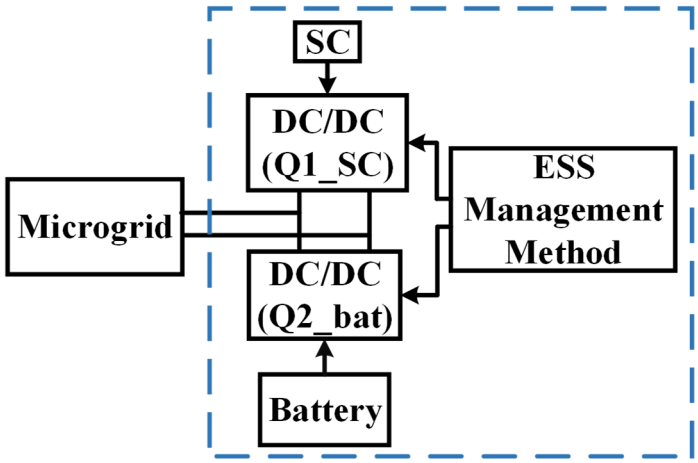

Fig. 3. Structure of the hybrid ESS.

2.1 The battery model

The Nickel-Cadmium battery model is employed in this work [31]. The main task for the BESS with the distributed energy sources power structure is storing the energy surplus produced by other resources and usage again usage it again when a shortage occurs for energy. The voltage of the battery in discharge/charge case is given by Eqs. (3) and (4), respectively [32]:

$$V_{batt} = E_0 - K(\frac{Q}{Q - i_b t})i^* - K(\frac{Q}{Q - i_b t})i_b t + Ae^{-B.it}(i^* > 0) \quad (3)$$

$$V_{batt} = E_0 - K(\frac{Q}{Q - i_b t})i^* - K(\frac{Q}{Q - i_b t})i_b t + Ae^{-B.it} (i^* < 0) \quad (4)$$

The fully charged state voltage and the exponential section voltage are calculated by Eqs, (3) and (4), respectively:

$$V_{full} = E_0 - Ri_b + A \quad (5)$$

$$V_{\exp} = E_0 - K(\frac{Q}{Q - Q_{\exp}})(Q_{\exp} + i_b) - Ri_b + Ae^{\frac{-3}{Q_{\exp}}Q_{\exp}} \quad (6)$$

and cell voltage of the nominal zone is expressed as:

$$V_{nom} = E_0 - K(\frac{Q}{Q - Q_{nom}})(Q_{nom} + i_b) - Ri + Ae^{\frac{-3}{Q_{nom}}Q_{nom}} \quad (7)$$

Also, the battery SOC is expected based on coulomb counting by collecting the capacity during the charge/discharge ($\eta = 1$ for discharge, and $\eta < 1$ for charge) case of the battery as:

$$SOC = SOC_0 - \frac{1}{Q_n}\int_0^t \eta i_b dt \quad (8)$$

Noted that, the battery SOC should be regulated between the safe bounds ($SOC_{\min} \le SOC \le SOC_{\max}$) in the actual positions.

2.2 The SC model

The block of SC applies a general model for presenting the widely used of SC in Fig. 3. The output voltage (V_{SC}) of SC is described as [33].

$$V_{SC} = \frac{N_{sc} Q_{ec} d}{N_{pc} N_e \varepsilon \varepsilon_0 A_i} + \frac{2N_e N_{sc} R_d T}{F} \sinh^{-1}\left(\frac{Q_{ec}}{N_{pc} N_e^2 A_i \sqrt{8R_d T \varepsilon \varepsilon_0 C_m}}\right) - R_{sc}.i_{sc} \quad (9)$$

$$Q_{ec} = \int i_{SC} dt \quad (10)$$

To present the self-discharge phenomenon, the SC charge equation is reformed as (when i_{SC} is 0):

$$Q_{ec} = \int i_{self\_dis} dt \tag{11}$$

Where,

$$i_{self\_dis} = \begin{cases} \dfrac{C_T \alpha_1}{1 + sR_{SC}C_T} & \text{if} \quad t - t_{OC} \le t_3 \\ \dfrac{C_T \alpha_2}{1 + sR_{SC}C_T} & \text{if} \quad t_3 < t - t_{OC} \le t_4 \\ \dfrac{C_T \alpha_3}{1 + sR_{SC}C_T} & \text{if} \quad t - t_{OC} \ge t_4 \end{cases} \tag{12}$$

The safe operating voltage of an SC will be as:

$$\left(v_{sc}\right)_{\min} < v_{sc} < \left(v_{sc}\right)_{\max} \tag{13}$$

In this study, the minimum and maximum operating voltage for SC is chosen as 240 and 380 v, respectively:

The value of the SC is predicted without considering wind turbine where it delivers the nominal power of microgrid, $P_{\text{microgrid}}$ (i.e., 460 kW) for supplying load at a time interval about 16 s. Consequently, the size of the SC is expressed as:

$$C_{\sup} = \frac{s_{\max} \times (P_{microgrid})_{reted} \times t}{\left[\left(V_{sc}\right)^2_{\max} - \left(V_{sc}\right)^2_{\min}\right]} \tag{14}$$

Using the Eq. (14) C_{sup} is obtained 20 F for this work study.

2.3 The SC-BESS combined model

The mathematical models of the battery and SC are simplified to make the analysis tractable. The equivalent circuit of the direct connection is displayed in Fig. 4(a), and its equivalent circuit in the Laplace domain and its Thevenin equivalent are presented in Fig. 4(b) and (c), respectively. The equivalent circuit is transformed into the frequency domain using the Laplace transform [34].

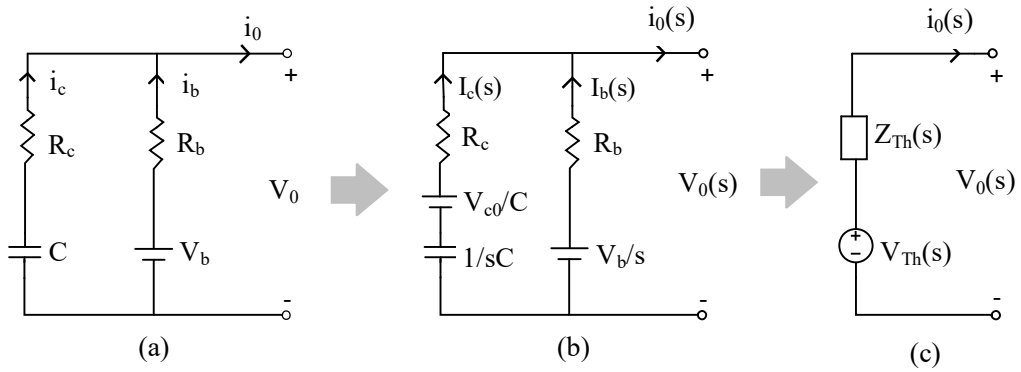

Fig. 4. Equivalent circuit of a SC in parallel connection with a battery ((a) Equivalent circuit of passive parallel connection (b) Equivalent circuit in the Laplace domain (c) Thevenin equivalent circuit).

$$V_{Th}(s) = V_b \frac{R_c}{R_b + R_c} \frac{s+\alpha}{s(s+\beta)} + V_{c0} \frac{R_b}{R_b + R_c} \frac{1}{s+\beta} \tag{15}$$

$$Z_{Th}(s) = (R_b + \frac{1}{sC}) \square R_b = \frac{R_b R_c}{R_b + R_c} \frac{s+\alpha}{s+\beta} \tag{16}$$

$$\alpha = \frac{1}{R_c C} \tag{17}$$

$$\beta = \frac{1}{(R_b + R_c)C} \tag{18}$$

Therefore, the inverse Laplace transform of the Thevenin voltage source in Eq. (15) leads to:

$$v_{Th}(t) = V_b + \frac{R_b}{R_b + R_C}(V_{c0} - V_b)e^{-\beta.t} \tag{19}$$

After achieving mathematical model of the Thevenin equivalent circuit, it is possible to connect a power charging source or load to this hybrid ESS. To analyze the behavior of hybrid

ESS when there is a charging source/load, suddenly fluctuating from one level to another, a pulsed source is assumed in this study. The analytical approach is presented as follows. The pulsed charging/load current with pulse duty ratio D and period T and for N pulses can be expressed as:

$$i_0(t) = I_0 \sum_{K=0}^{N-1} \left[\Phi(t - kT) - \Phi(t - (k + D)T \right] \tag{20}$$

By operating the Laplace transform on Eq. (20), the current in the frequency domain is:

$$I_0(s) = \sum_{k=0}^{N-1} \left[\frac{e^{-kT.s}}{s} - \frac{e^{-(k+D)T.s}}{s} \right] \tag{21}$$

For the given form of charging current, the internal voltage drop $V_i(s)$ in Fig. 4(c) is:

$$V_i(s) = Z_{Th} I_0(s) \tag{22}$$

Through an inverse Laplace transform, the corresponding expression in the time domain is:

$$v_i(t) = R_b I_0 \sum_{k=0}^{N-1} \left\{ \left(1 - \frac{R_b}{R_b + R_c} e^{-\beta(t-kT)} \right) \Phi(t - kT) \right.$$
$$\left. -(1 - \frac{R_b}{R_b + R_c} e^{-\beta[t-(k+D)T]} \times \Phi\left[t - (k + D)T \right] \right\} \tag{23}$$

From the circuit in Fig. 4c, the output/power source voltage can be expressed as:

$$V_0(s) = V_{Th}(s) - V_i(s) \tag{24}$$

By combining Eqs. (19) and (23), the above Eq. (24) in the time domain can be expressed as:

$$v_0(t) = v_{Th}(t) - v_i(t) = V_b + \frac{R_b}{R_b + R_c} (V_{c0} - V_b) e^{-\beta.t}$$
$$-R_b I_0 \sum_{k=0}^{N-1} \left\{ \left(1 - \frac{R_b}{R_b + R_c} e^{-\beta(t-kT)} \right) \Phi\left(t - kT \right) \right.$$
$$\left. -\left(1 - \frac{R_b}{R_b + R_c} e^{-\beta\left[t-(k+D)T \right]} \right) \times \Phi\left[t - \left(k + D \right)T \right] \right\} \tag{25}$$

Finally, the currents in the battery and SC can be derived based on the resolved output/power source voltage in Eq. (25):

$$i_b(t) = \frac{1}{R_b}\left[V_b - v_0(t)\right] \tag{26}$$

$$i_c(t) = i_0(t) - i_b(t) \tag{27}$$

If the battery voltage reaches to SC voltage, a steady state exists, i.e. $V_{0c} = V_b$. The battery voltage can then be found using Eqs. (25) and (26):

$$i_{bss}(t) = I_0 \sum_{k=0}^{N-1} \left\{ (1 - \frac{R_b}{R_b - R_c} e^{-\beta(t-kT)}) \Phi(t-kT) \right.$$
$$\left. -(1 - \frac{R_b}{R_b - R_c} e^{-\beta[t-(k+D)T]}) \times \Phi\left[t-(k+D)T\right] \right\} \tag{28}$$

Similarly, the SC current under steady state conditions is:

$$i_{scc}(t) = \frac{R_b I_0}{R_b + R_c} \sum_{k=0}^{N-1} \left\{ e^{-\beta(t-kT)} \Phi(t-kT) - e^{-\beta[t-(k+D)T]} \Phi\left[t-(k+D)T\right] \right\} \tag{29}$$

Based on Eq. (28), the peak current of battery appears at the end of the pulsed charging current, i.e. $t = (k + D)\ T$. With time increasing, n tends toward infinity, and the expression for peak battery current is:

$$I_{bpeak} = I_0 \left[1 - \frac{R_b e^{-\beta DT}}{R_b - R_c} \frac{1 - e^{-\beta(1-D)T}}{1 - e^{-\beta DT}} \right] = I_0 (1 - \zeta_c) \tag{30}$$

where ζ_c is the current sharing factor of the SC at the peak charging current:

$$\zeta_c = \frac{R_b}{R_b - R_c} \frac{e^{-\beta DT}(1 - e^{-\beta(1-D)T})}{1 - e^{-\beta DT}} \tag{31}$$

3. Control of the microgrid

As well known, wind energy is not accessible for all time, and its action is affected by random weather conditions. Thus, the distributed sources generated energy is not always identical to the consumer demanded energy. For continuous accessibility of energy in modern systems, the storage unit is an essential tool, especially in the development of wind energy. However, for management of active power a useful control mechanism is necessary among different resources. The DOFCS controller as introduced in Fig. 5 is implemented in this system. It has two parts: a conventional discrete PD controller and a fuzzy logic unit. The PD part is applied to cope with fast variation and large overshoots in input of the control unit due to the load and wind power changes. Due to Fig. 5, in an intelligent fuzzy system unit the nominal frequency and synchronous speed in *pu* is used as inputs to online adjust of the PD parameters. The next step is creating a rule table and membership function for fuzzy logic. The fuzzy rules sets are shown in Table 2. The corresponding membership functions for the input and output variables are arranged as triangular function.

Optimally adjusting all gains of the fuzzy type DOCS controller *i.e.*: K_d, K_i, K_p, α and β, has a key role to obtain good performance capabilities under load and wind power variations. A PSO technique is applied to decrease fuzzy system effort and cost. The motivation for this problem is a combination of the fuzzy theory features and PSO algorithm to reduce control efforts and find a better DCS system to achieve the robust power quality in the isolated microgrid. This control mechanism has a flexible structure and easy to implement.

It should be noted that the fuzzy controller performance highly depends on the membership functions. Without precise information about the system, the membership functions cannot be carefully selected, and the designed fuzzy controller does not provide optimal performance in a wide range of operating conditions. Therefore, a complementary algorithm is used to online regulating of membership functions [35]. In the proposed control strategy, the DOFCS

parameters are automatically tuned using fuzzy rules, according to the online measurements. In order to obtain an optimal performance, the PSO technique is used as offline to determine the membership functions parameters.

Also, noted that the proper choice of the cost function has a key role in synthesis procedure. Hence, the following cost function is introduced for optimization:

$$J = \int_0^{T_s} (\Delta f_m{}^2 + \Delta P_m{}^2) \tag{32}$$

Where, T_s is the simulation time, Δf_m and ΔP_m are frequency (e_f) and generated power deviations (e_P) of microgrid (Fig. 2 and Fig. 5). The optimized values of controller gains values are given in Appendix A.

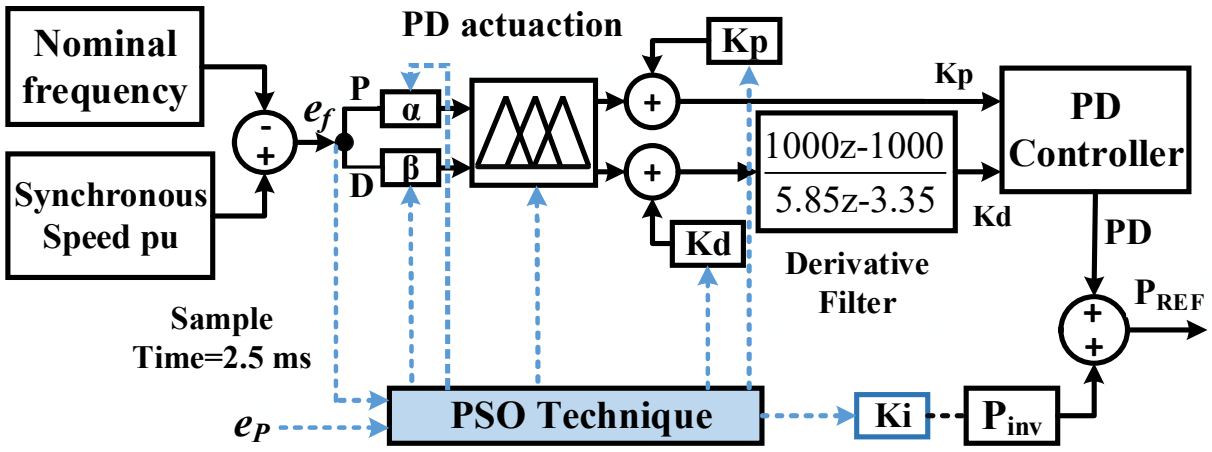

Fig. 5. Structure of the proposed DOFCS control strategy.

Table 2. The fuzzy rules set.

e/Δe	NB	NS	Z	PS	PB
NB	BG	BG	MD	BG	BG
NS	BG	MD	SM	MD	BG
Z	MD	SM	SM	SM	BG
PS	BG	MD	SM	MD	BG
PB	BG	BG	MD	BG	BG

Negative Big (NB), Negative Medium (NM), Negative Small (NS), Zero (Z), Positive Small (PS), Positive Medium (PM) and Positive Big (PB)

4. Management of the hybrid SC-BESS storage

Here, an algorithm is provided for management of energy in the hybrid SC-BESS storage unit to accomplish the following tasks:

1) Balancing active power between the microgrid generation units, ESSs and loads,
2) Preventing from the deep charging/discharging in the battery,
3) Enhancing the effectiveness of the BESS, and
4) Decreasing the demand of peak power, the battery charging/discharging cycle, and dynamic stress level.

The conventional BESS is capable to store and deliver continuous power to the load. The high energy density characteristic of the batteries makes them a suitable choice for steady power supply. However, supplying a large burst of current from the battery reduces its lifetime. An alternative solution is a combination of batteries with high power density source capable of supplying the burst transient current such as a SC. In such hybrid systems, the battery fulfills the supply of continuous energy while the SC supplies transient power for system load. However, a proper energy management technique is necessary for this hybrid storage system. For this reason, an energy management method as shown in Fig. 6 is applied to control the supply and storage of energy throughout the system. First, the fluctuating parts are removed by the low-pass filter from the signal applied to ESS. A regulator (PI controller), limiter, and low-pass filter are used to determine the charging/discharge current and then the charge/discharge status of the SC/battery. Once the bus voltage droplets under the reference voltage, the voltage regulator orders the battery to be charged. This signal is applied to the limiting block so that the discharge current does not exceed the limit set for the battery. Q1_SC and Q2_bat are linked to the DC-DC converter of Fig 3 (Hybrid ESS). The purpose of this management approach is to smooth battery current from the sudden changes during the charging/discharging mode.

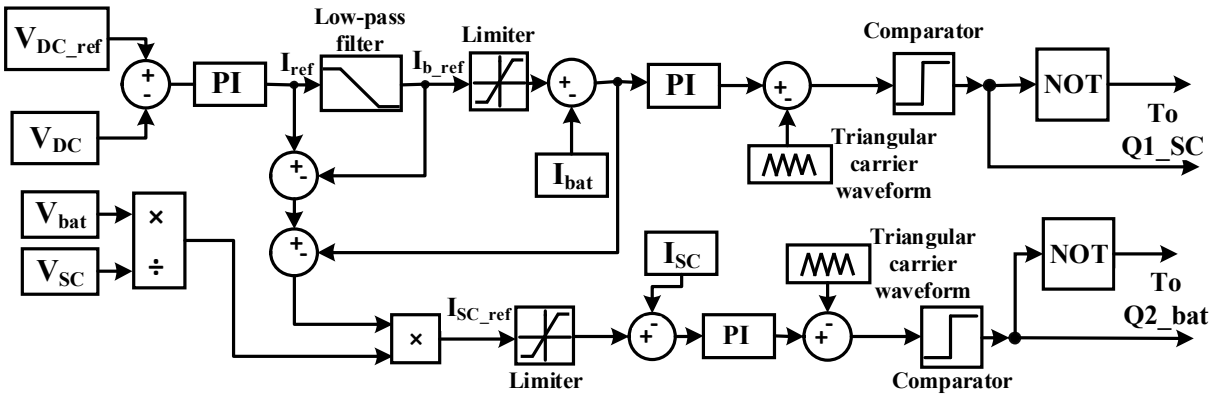

Fig. 6. Management method for energy of the hybrid SC-BESS unit.

In general, Fig. 7 presents the implementation flowchart of the proposed method. This process has three stages: (i) processing stage, (ii) management/control part and (iii) post processing part.

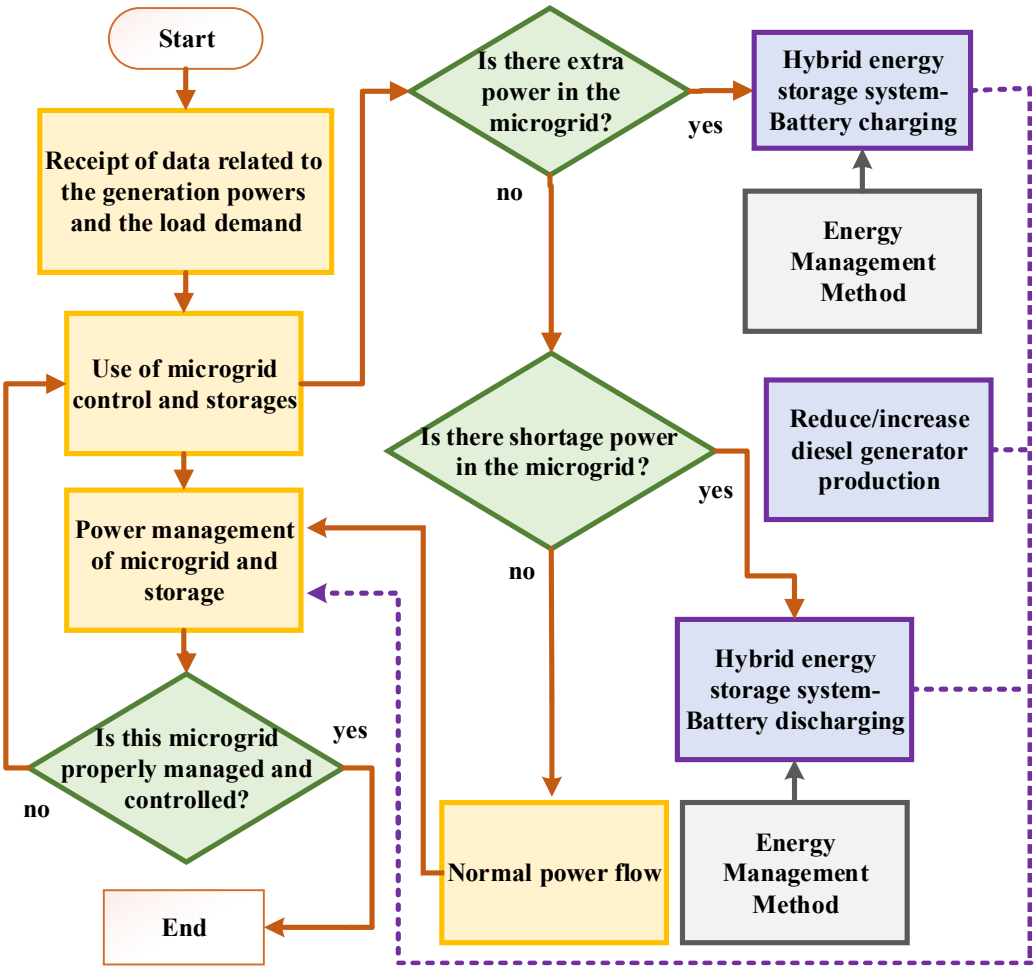

Fig. 7. The implementation flowchart of the proposed method.

5. Results and Discussions

Here, the effectiveness of the suggested fuzzy type DCS and hybrid energy storage system is verified on an islanded wind-diesel power system as shown in Fig. 1 against wind speed and consumer load variants. The data is given in Appendix A [23]. Note that when the wind speed is high, diesel generator goes to product minimum power and hence, the BESS begins to charge, because the production power is more than the demand of system load and vice versa.

Figure 8 shows the variation of WTG, SG, BESS and consumer load active power under two operation conditions. In the first case (0.2 to 8.2 s) the extra load (-125 kW) is applied to the system at 0.2 s and in the second case the wind speed is changed from its nominal value of 7 to 10 m/s at 8.2 s. Although, there is a wide variation in system consumer load at the time interval 0.2-2 s, whereby these transient load changes are compensated using DG and BESS (the highest efficiency of DG is considered to be up to 95 kW).

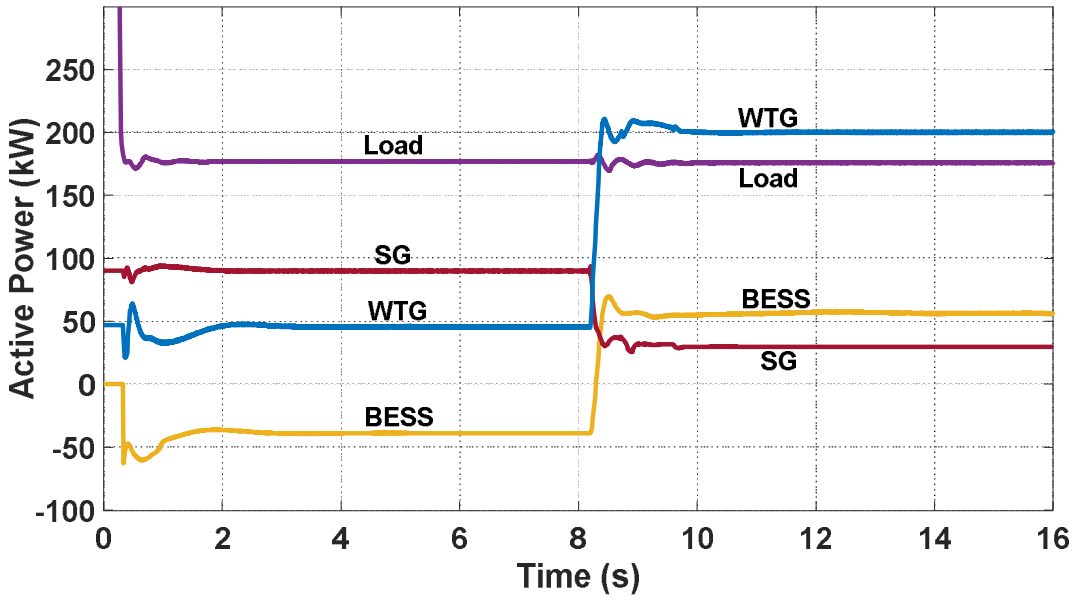

Fig. 8. The active power variation of WTG, SG, BESS and consumer load.

In the steady state, the total produced power by WTG and SG is 135 kW, while the requested power is 175 kW. Hence, the rest of the system load (40 kW) is compensated by the BESS. In the second case (8.2 s to 16 s), wind turbine power is increased and exceeded from the microgrid

demand. In this case, the total produced power by WTG and SG is 230 kW, while the requested power is 175 kW. Because of this, the generated power of the DG is reduced and when it is reached at lower than of 30 kW, its reverses power protection is activated, since the least stable operation of DG is considered to be 30 kW. Also, the BESS is started to charge and extra produced power is stored through it.

Figure 9 (a) and (b) depict isolated system voltage under two mentioned operating conditions in the above. Using the command of the proposed DOFCS, a good regulation is achieved with significantly reducing overshoot/undershoot than the DCS controller one [23] in both cases.

Isolated system frequency is illustrated in Fig. 10 when system load changes are applied at 0.2 s (first case) and wind speed increased at 8.2 s using the following three strategies.

i) With BESS and DCS controller [23]

ii) With the proposed hybrid SC/BESS and DCS controller

iii) With the proposed hybrid SC/BESS and DOFCS controller

It can be concluded that the frequency deviations of the isolated power system are properly improved from the system transient behavior such as settling time and overshoot/undershoot using the proposed hybrid SC/BESS and DOFCS in comparison with other ones.

The dynamics behaviors of the battery current with/without SC are shown in Fig. 11. At the time interval of 0.2 to 1.9 s, the battery is smoothly discharged than the case no SC is applied. In addition, the result shows that by making of SC and the proposed management algorithm, the battery peak current is decreased from about -290 A to -275 A during the consumer load step changes and from about 340 A to 290 A under wind power variation case.

The transient behavior of the battery current is shown in Table 3. It is indicated that using the proposed strategy the overshoot is improved about 28.15% and 381.66% in the first and second cases, respectively. Thus, the pressure on the battery is significantly decreased in the transient

state which is caused to increase battery lifetime. Moreover, the battery and SC electric variables are shown in Figs. 12-13. It can be seen that the proposed methodology has good effectiveness.

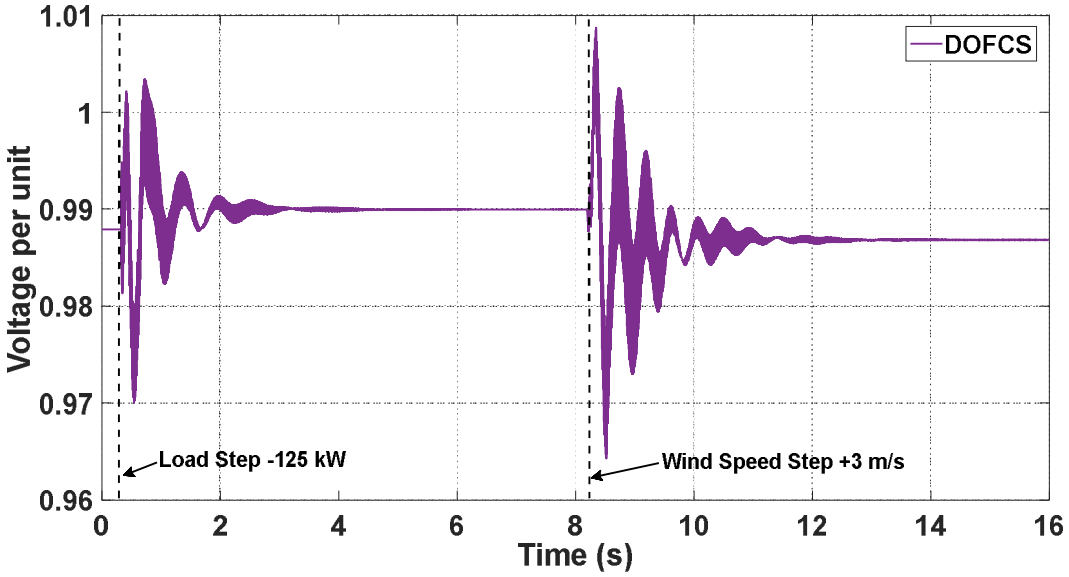

(a)

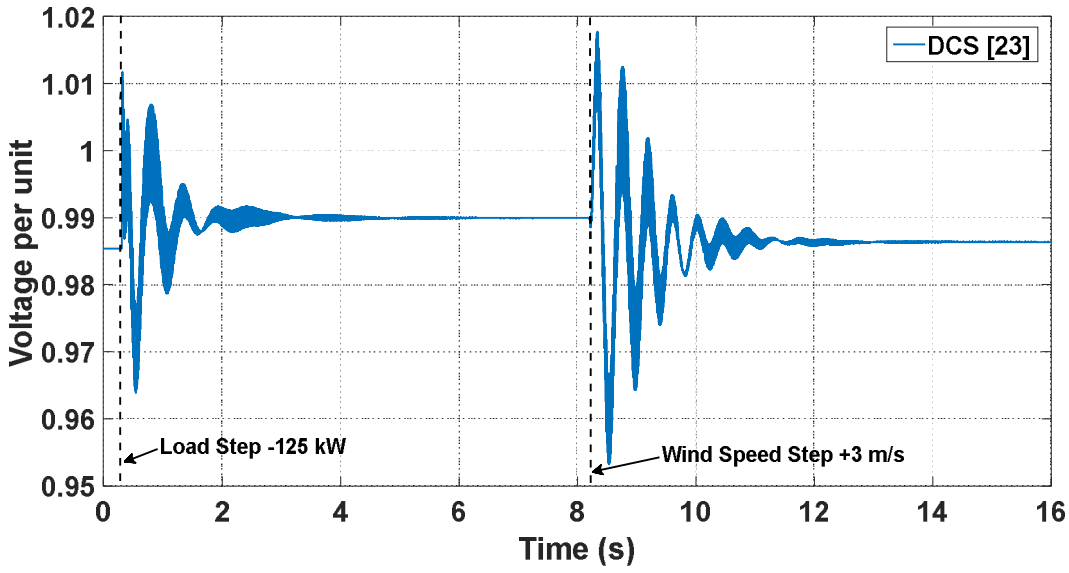

(b)

Fig. 9. System voltage.

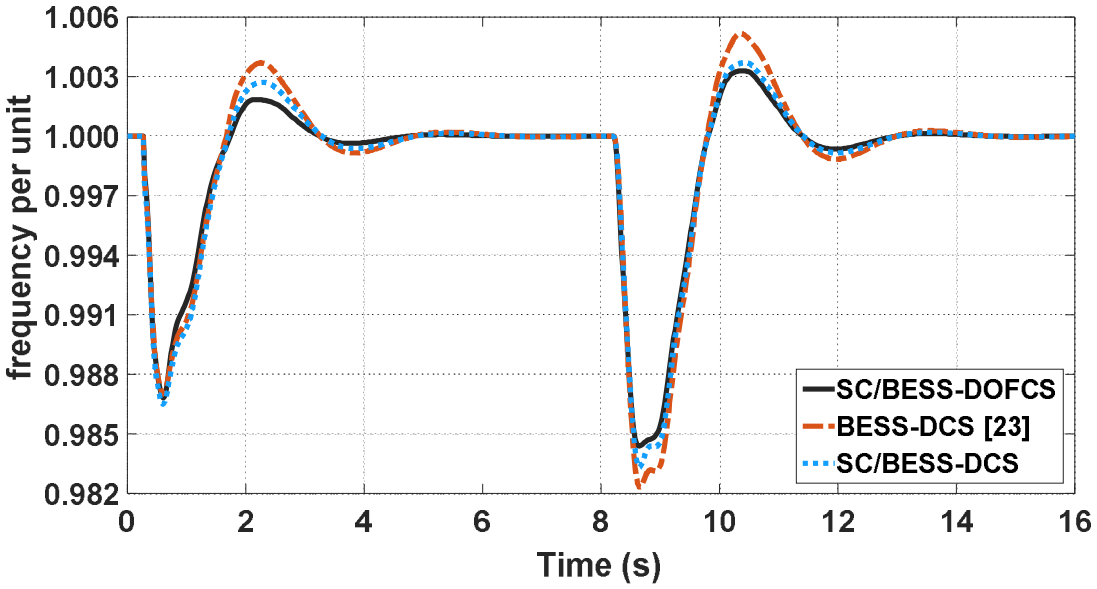

Fig. 10. System frequency.

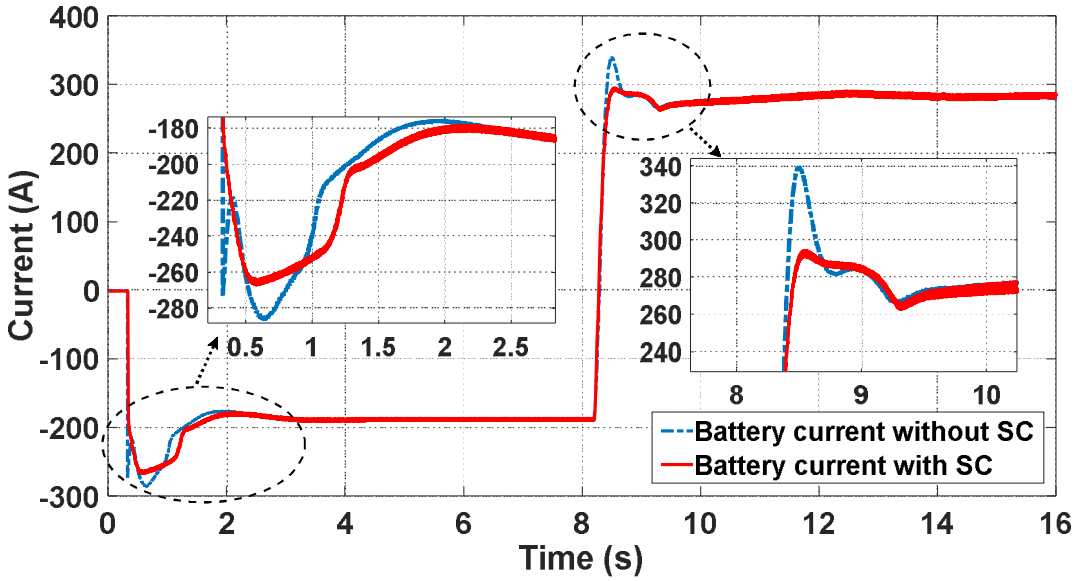

Fig. 11. The behaviors of the battery currents with and without SC.

Table 3. Maximum overshoot (OS) of the battery current for two operating conditions

Parameter/case	First case	Second case
OS value without SC	96.5 A	57.8 A
OS value with SC	75.3 A	12 A
OS Improvement	28.15 %	381.66 %

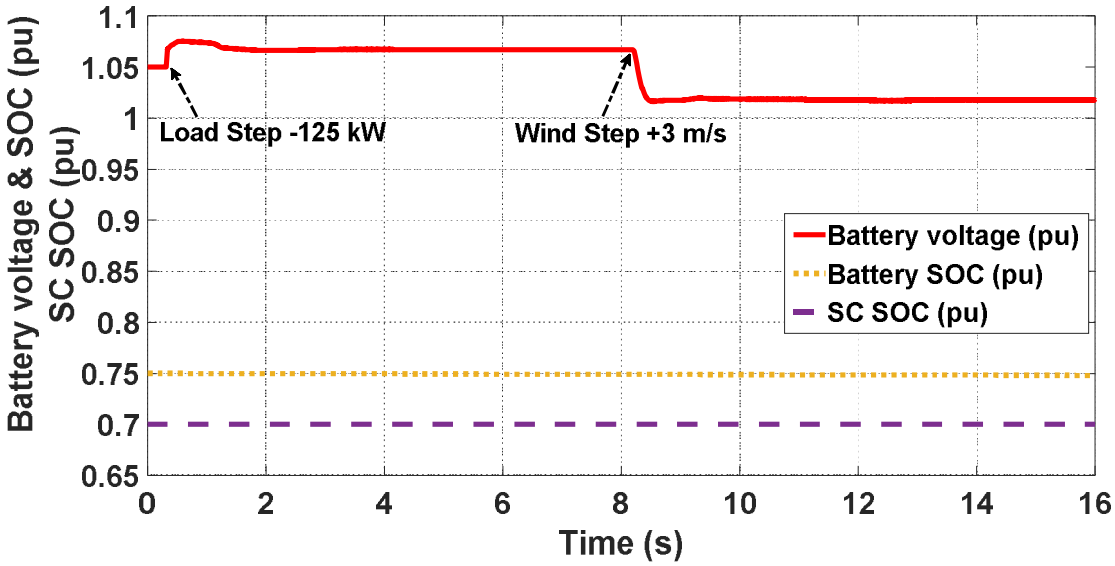

Fig. 12. Battery voltage (pu), battery SOC (pu) and SC SOC (pu).

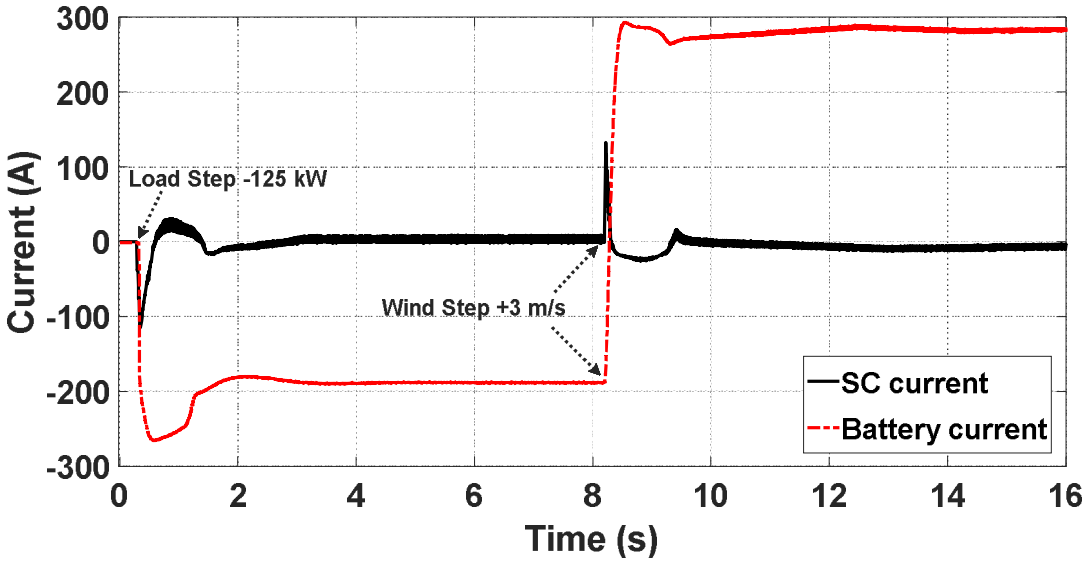

Fig. 13. Currents of battery and SC.

6. Conclusion

This paper has addressed the islanded operation of a wind-diesel power system using the DOFCS and a hybrid ESS consisting of a battery energy storage and SC. The energy balance operation imposes severe stress on the battery if it is solely used as an energy storage system, because the battery has low power density. Thus, a high power density system i.e. SC combined with a BESS was proposed using a suitable control approach to share the active power imbalance between the system power resources and consumer loads. The entire system was simulated under

extreme operating conditions such as the consumer load and wind speed step changing. The proposed fuzzy type DSC can be enabled to enable the hybrid SC-BESS for a suitable balancing of active power under consumer load fluctuations as well as those of the wind power variations, thus efficiently regulating system frequency/voltage dynamics and enhancing the wind-diesel hybrid system power quality.

Acknowledgment

J.P.S. Catalão acknowledges the support by FEDER funds through COMPETE 2020 and by Portuguese funds through FCT, under POCI-01-0145-FEDER-029803 (02/SAICT/2017).

References

[1] A. Elmitwally and M. Rashed, "Flexible operation strategy for an isolated PV-diesel microgrid without energy storage," *IEEE transactions on energy conversion,* vol. 26, pp. 235-244, 2010.

[2] "Wind/Diesel Systems Architecture Guidebook," *American Wind Energy Association,* 1991.

[3] C. Cho, J.-H. Jeon, J.-Y. Kim, S. Kwon, K. Park, and S. Kim, "Active synchronizing control of a microgrid," *IEEE Transactions on Power Electronics,* vol. 26, pp. 3707-3719, 2011.

[4] G. Delille, B. Francois, and G. Malarange, "Dynamic frequency control support by energy storage to reduce the impact of wind and solar generation on isolated power system's inertia," *IEEE Transactions on sustainable energy,* vol. 3, pp. 931-939, 2012.

[5] H. Shayeghi, A. Jalili, and H. Shayanfar, "Multi-stage fuzzy load frequency control using PSO," *Energy conversion and management,* vol. 49, pp. 2570-2580, 2008.

[6] H. Shayeghi and A. Younesi, "Mini/Micro-Grid Adaptive Voltage and Frequency Stability Enhancement," *Journal of Operation and Automation in Power Engineering,* vol. 7, pp. 107-118, 2019.

[7] H. Shayeghi and A. Younesi, "Enhancement of Voltage/Frequency Stability in an Autonomous Micro Energy Grid with Penetration of Wind Energy Using a Parallel Fuzzy Mechanism," *Iranian Journal of Electrical and Electronic Engineering,* in press, 2020.

[8] W. Gu, W. Liu, Z. Wu, B. Zhao, and W. Chen, "Cooperative control to enhance the frequency stability of islanded microgrids with DFIG-SMES," *Energies,* vol. 6, pp. 3951-3971, 2013.

[9] P. Kou, F. Gao, and X. Guan, "Stochastic predictive control of battery energy storage for wind farm dispatching: Using probabilistic wind power forecasts," *Renewable Energy,* vol. 80, pp. 286-300, 2015.

[10] J. Hu, Y. Shan, Y. Xu, and J. M. Guerrero, "A coordinated control of hybrid ac/dc microgrids with PV-wind-battery under variable generation and load conditions," *International Journal of Electrical Power & Energy Systems,* vol. 104, pp. 583-592, 2019.

[11] R. Dufo-Lopez, I. R. Cristobal-Monreal, and J. M. Yusta, "Stochastic-heuristic methodology for the optimisation of components and control variables of PV-wind-diesel-battery stand-alone systems," *Renewable Energy,* vol. 99, pp. 919-935, 2016.

[12] A. Schneuwly, "High reliability power backup with advanced energy storage (white paper)," *Maxwell Technologies, San Diego, CA, USA" Tech. Rep.,* 2006.

[13] Q. Xu, X. Hu, P. Wang, J. Xiao, P. Tu, C. Wen*, et al.*, "A decentralized dynamic power sharing strategy for hybrid energy storage system in autonomous DC microgrid," *IEEE transactions on industrial electronics,* vol. 64, pp. 5930-5941, 2016.

[14] R. Sebastián, "Application of a battery energy storage for frequency regulation and peak shaving in a wind diesel power system," *IET Generation, Transmission & Distribution,* vol. 10, pp. 764-770, 2016.

[15] G. Pathak, B. Singh, and B. K. Panigrahi, "Back-propagation algorithm-based controller for autonomous wind–DG microgrid," *IEEE Transactions on Industry Applications,* vol. 52, pp. 4408-4415, 2016.

[16] C. Abbey and G. Joos, "Short-term energy storage for wind energy applications," in *Fourtieth IAS Annual Meeting. Conference Record of the 2005 Industry Applications Conference, 2005.*, 2005, pp. 2035-2042.

[17] A. Esmaili, B. Novakovic, A. Nasiri, and O. Abdel-Baqi, "A hybrid system of li-ion capacitors and flow battery for dynamic wind energy support," *IEEE Transactions on industry applications,* vol. 49, pp. 1649-1657, 2013.

[18] N. Mendis, K. Muttaqi, and S. Perera, "Management of low-and high-frequency power components in demand-generation fluctuations of a DFIG-based wind-dominated RAPS system using hybrid energy storage," *IEEE Transactions on Industry Applications,* vol. 50, pp. 2258-2268, 2013.

[19] X. Xiao, H. Yi, Q. Kang, and J. Nie, "A two-level energy storage system for wind energy systems," *Procedia environmental sciences,* vol. 12, pp. 130-136, 2012.

[20] B. Hredzak, V. G. Agelidis, and M. Jang, "A model predictive control system for a hybrid battery-ultracapacitor power source," *IEEE Transactions on Power Electronics,* vol. 29, pp. 1469-1479, 2013.

[21] M.-E. Choi, S.-W. Kim, and S.-W. Seo, "Energy management optimization in a battery/supercapacitor hybrid energy storage system," *IEEE Transactions on Smart Grid,* vol. 3, pp. 463-472, 2011.

[22] L. W. Chong, Y. W. Wong, R. K. Rajkumar, and D. Isa, "An optimal control strategy for standalone PV system with Battery-Supercapacitor Hybrid Energy Storage System," *Journal of Power Sources,* vol. 331, pp. 553-565, 2016.

[23] R. Sebastián, "Reverse power management in a wind diesel system with a battery energy storage," *International Journal of Electrical Power & Energy Systems,* vol. 44, pp. 160-167, 2013.

[24] J. M. Lujano-Rojas, C. Monteiro, R. Dufo-López, and J. L. Bernal-Agustín, "Optimum load management strategy for wind/diesel/battery hybrid power systems," *Renewable Energy,* vol. 44, pp. 288-295, 2012.

[25] A. Haruni, A. Gargoom, M. E. Haque, and M. Negnevitsky, "Dynamic operation and control of a hybrid wind-diesel stand alone power systems," in *2010 Twenty-Fifth Annual IEEE Applied Power Electronics Conference and Exposition (APEC)*, 2010, pp. 162-169.

[26] T.-L. Pan, H.-S. Wan, and Z.-C. Ji, "Stand-alone wind power system with battery/supercapacitor hybrid energy storage," *International Journal of Sustainable Engineering,* vol. 7, pp. 103-110, 2014.

[27] Y. Y. Chia, L. H. Lee, N. Shafiabady, and D. Isa, "A load predictive energy management system for supercapacitor-battery hybrid energy storage system in solar application using the Support Vector Machine," *Applied Energy,* vol. 137, pp. 588-602, 2015.

[28] M. Sarvi and I. N. Avanaki, "An optimized fuzzy logic controller by water cycle algorithm for power management of stand-alone hybrid green power generation," *Energy conversion and management,* vol. 106, pp. 118-126, 2015.

[29] R. Cozzolino, L. Tribioli, and G. Bella, "Power management of a hybrid renewable system for artificial islands: A case study," *Energy,* vol. 106, pp. 774-789, 2016.

[30] M. Jayachandran and G. Ravi, "Predictive power management strategy for PV/battery hybrid unit based islanded AC microgrid," *International Journal of Electrical Power & Energy Systems,* vol. 110, pp. 487-496, 2019.

[31] "Implement generic battery model [Online]." Available: http://www.mathworks.com.au/help/physmod/powersys/ref/battey.hml.

[32] L. Saw, K. Somasundaram, Y. Ye, and A. Tay, "Electro-thermal analysis of Lithium Iron Phosphate battery for electric vehicles," *Journal of Power Sources,* vol. 249, pp. 231-238, 2014.

[33] A. A. Elbaset, S. A. M. Abdelwahab, H. A. Ibrahim, and M. A. E. Eid, "The Performance Analysis of a PV System with Battery-Supercapacitor Hybrid Energy Storage System," in *Performance Analysis of Photovoltaic Systems with Energy Storage Systems*, ed: Springer, 2019, pp. 75-99.

[34] T. Ma, H. Yang, and L. Lu, "Development of hybrid battery–supercapacitor energy storage for remote area renewable energy systems," *Applied Energy,* vol. 153, pp. 56-62, 2015.

[35] H. Bevrani, F. Habibi, P. Babahajyani, M. Watanabe, and Y. Mitani, "Intelligent frequency control in an AC microgrid: Online PSO-based fuzzy tuning approach," *IEEE transactions on smart grid,* vol. 3, pp. 1935-1944, 2012.

Appendix

Parameters

Islanded Power System:
F=60 Hz, Nominal voltage =480 V

DG:
Inertia constant of DG, H_{DG}=1.75 s, $P_{SG\text{-}NOM}$=300 kVA

WTG:
$P_{T\text{-}NOM}$ =275 kW, Inertia constant of WTG, H_{WTG}=2 s

APR:
$f_{sampling}$=400 Hz; K_P=90.1721, K_D=6.3011 kWs/Hz, Reverse Power Integral gain=8.6011 s^{-1}; α=0.3337; β=0.4971;

Converter:
V_{L-L}=120 V, $P_{S\text{-}NOM}$ =150 kW

Battery:
Battery rated Capacity = 390.625 Ah, Battery rated Voltage = 240 v, Battery rated Current = 625 A (150 kW/240 V = 625 A)

Transformer:
S=150 kVA, 480/120 V;

SC:
C=20 F